THE JOURNAL OF PHYSICAL CHEMISTRY B

Article

pubs.acs.org/JPCB

Interaction of Thionine with Triple-, Double-, and Single-Stranded RNAs

Héctor J. Lozano, Begoña García,* Natalia Busto, and José M. Leal

Chemistry Department, University of Burgos, 09001 Burgos, Spain

Supporting Information

ABSTRACT: The interaction of thionine with triple, double, and single RNA helices has been fully characterized by thermodynamic and kinetic methods. The nature of the interaction of thionine with the synthetic polynucleotides poly(rU), poly(rA)·poly(rU), and poly(rA)·2poly(rU) has been studied at pH = 7.0 and 25 °C by UV absorbance, fluorescence, circular dichroism spectroscopy, viscometry, differential scanning calorimetry, and T-jump kinetic measurements. The results show that at I = 0.1 M thionine binds to a single poly(rU) strand, destabilizes the poly(rA)·2poly(rU) triplex by external binding, and intercalates into poly(rA)·poly(rU) with similar affinity to the thionine/DNA intercalated complex (Paul, P.; Kumar, G. S. *J. Fluoresc.* **2012**, *22*, 71−80). On the other hand, the differential scanning calorimetry measurements performed with thionine display a point in which the heat capacity remains unaltered, revealing the equilibrium of isothermal denaturation: thionine/poly(rA)·2poly(rU) + thionine ⇌ thionine/poly(rA)·poly(rU) + thionine/poly(rU), an outcome supported by the other techniques used. The denaturation equilibrium constant, K_D (25 °C) = 522 M^{-1}, was evaluated from the affinity with the single, duplex, and triplex RNA.

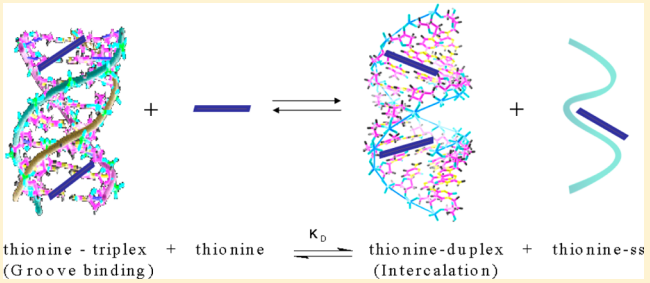

1. INTRODUCTION

The biological activity of acridine derivatives as mutagens, antimicrobial, antimalarial, or bactericide agents is related to their nucleic acids binding properties.[2] Thionine (3,7-diamino-5-phenothiazinium), Figure 1, a fully planar tricyclic heteroatomic derivative with two amine groups at the C3 and C7 sites,[3] is monocationic under physiological conditions, and it has been studied because of its intercalative binding with DNA.

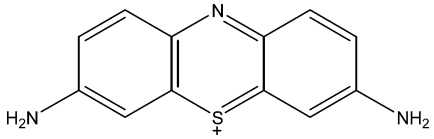

Figure 1. Thionine (3,7-diamino-5-phenothiazinium).

Thionine has been used to induce photodynamic inactivation of bladder cancer cells, *Escherichia coli*, and *Saccharomyces cerevisiae*.[4] Previous studies have revealed mutagenic activity in eukaryotic cells,[5] demonstrating also potential cytotoxic and genotoxic activity in prokaryotic cells and photoinduced mutagenic action upon binding to DNA.[6] The biological activity of thionine has also been employed in graphene-based inmunosensors.[7] Thionine interacts with double-stranded DNA and, to less extent, with single-stranded DNA via intercalation,[1,8] showing a pronounced preference for the alternating GC sequences followed by the polyG·polyC sequences.[9] Recently, theoretical analyses of the binding of thionine with *Clostridium perfringenes* (CP) DNA duplex have been reported to explain the melting behavior and heat capacity of this system. Growing interest has emerged in polynucleotide structures different from typical double helices, which may play important roles in biology; in this regard, thionine has been shown to bind quadruplex structures via external stacking.[10] These and other interesting properties of thionine are explained by the molecular features of its interaction with nucleic acids. The elucidation of the molecular aspects of the interaction of aromatic molecules with DNA and RNA has been the subject of investigation since the discovery of these structures. Despite all these studies, little is known about the thionine binding to RNA.

RNA is involved in a number of processes in the regulation of gene expression and can adopt numerous structures and conformations, displaying several cell functions and consequently providing specific binding sites for small molecules.[11,12] These conformations offer attractive potential targets for drugs able to bind specifically to such structures and can inhibit the viral transcription.[13]

To gain a better knowledge of RNA-based small-molecule therapeutics, a detailed study of the drug interaction to various RNA conformations, single-, double-, and triple-stranded, is undertaken here. The homopolymer poly(rA)·poly(rU) consists of two poly(rA) and poly(rU) attached chains to give a secondary structure with an endo fold at C3 of furanose rings.[14]

Received: August 7, 2012
Revised: November 28, 2012
Published: December 3, 2012

   dx.doi.org/10.1021/jp307840c | *J. Phys. Chem. B* 2013, 117, 38−48

Its interaction with different ligands has relevance in the research of both the alteration of protein synthesis[15] and the potential use as biological agent in the anticancer and antiviral therapy.

Triple helices have received a deal of attention as potential tools to control the gene expression[16,17] and represent attractive targets for antisense[18] and antigene-based[19] therapeutic strategies. Stabilization of triple-helical structures can be attained by intercalators,[13,20,21] especially covalently linked to the third strand,[22,23] whereas intercalators not covalently linked can either stabilize[24] or destabilize[25] triple-helix structures. The poly(rA)·2poly(rU) RNA triplex helix is essentially a poly(rA)·poly(rU) double helix with a poly(rU) chain inserted into the major groove and was first reported by Felsenfeld et al. in 1957.[26] The adenine groups of the third strand bind uracil groups in the same way as in viral genomes and mRNA.[14] It has been reported that poly(rA)·2poly(rU) becomes destabilized upon addition of ethidium bromide (EB) to such an extent that, at high dye-to-polymer ratio, the triple-strand structure can be destroyed.[27] A minor destabilizing effect was observed with proflavine, in which the binding is intercalative at low dye-to-polymer ratio, whereas the external binding dominates at high ratio.[28] We have reported earlier new aspects on the interaction of the antibiotic coralyne, which induces the formation of triple helix in poly(rA)·poly(rU).[29] Comparison of the binding of the same drugs with duplex and triplex reveals that insertion of the third strand into the major groove plays a key role in the kinetic and thermodynamic behavior. In general, the activity of the dye is the result of a set of variables such as dye geometry or protons adjacent to polynucleotide chains and functional groups.[30] The behavior of thionine with different synthetic RNA conformations (poly(rU), poly(rA)·poly(rU), and poly(rA)·2poly(rU)) is studied here to determine whether thionine selectively recognizes the RNA conformation and to learn the interactional affinity and the underlying mechanism of binding. Attention is focused on the characterization of the binding processes and conformational changes induced by thionine using a combination of static and dynamic methods.

2. MATERIALS AND METHODS

Thionine acetate, poly(rA)·poly(rU), and poly(rU) were purchased from Sigma-Aldrich. Doubly distilled water from a Millipore Q apparatus (APS, Los Angeles, California) was used. Stock solutions were prepared in [NaCl] = 0.01 or 0.1 M, using 2.5×10^{-3} M sodium cacodylate [$(CH_3)_2AsO_2Na$] as a buffer to maintain the pH at 7.0. The polynucleotide concentration was evaluated spectrophotometrically at λ = 260 nm using ε = 14 900 M^{-1} cm^{-1} for poly(rA)·poly(rU) and ε = 8900 M^{-1} cm^{-1} for poly(rU).[31] Poly(rA)·2poly(rU) was prepared by mixing equimolar amounts of poly(rA)·poly(rU) and poly(rU) and incubating the mixture at 25 °C for 24 h, a time range in which the triple helix is formed. The polynucleotide concentration, C_P, is expressed in molarity of base pairs for poly(rA)·poly(rU) and base triplets for poly(rA)·2poly(rU). The thionine concentration is denoted as C_D. pH measurements were carried out with a Metrohm 16 DMS Titrino pH meter, fitted with a combined glass electrode with a 3 M KCl solution as a liquid junction.

Spectrophotometric measurements were performed with a Hewlett-Packard 8453A (Agilent Technologies, Palo Alto, CA) photodiode array spectrophotometer with a Peltier temperature control system. Titrations were carried out by adding increasing amounts of polynucleotide solutions to the thionine solution in the cell. The sample was not illuminated during the equilibration period. Titrations were performed at 25 °C and analyzed at λ = 600 nm. The data were corrected for dilution (C°_D/C_D). Thermal denaturation studies were carried out by heating the dye/polynucleotide solution from 20 to 90 °C at 0.2 °C/min scan rate. The system was allowed to equilibrate for at least 1 min before measurements.

Spectrofluorimetric measurements: fluorescence titrations were performed on a Shimadzu Corporation RF-5301PC spectrofluorometer (Duisburg, Germany) at λ_{ex} = 565 nm and λ_{em} = 620 nm. The titrations were carried out as described for absorbance titrations. Fluorescence quenching measurements were obtained using $K_4[Fe(CN)_6]$ 1×10^{-2} M as a quencher. Measurements were performed by adding increasing amounts of $K_4[Fe(CN)_6]$ solution directly to the cell containing the dye and dye/polynucleotide system.

Differential scanning calorimetry (DSC): thermal denaturation studies were performed with a nano DSC (TA Instruments, Newcastle, U.S.A.). Cells were 300 μL platinum capillary tubes. Measurements were performed by heating the dye/polynucleotide system from 20 to 90 °C, at 1 °C/min scan rate and 3 atm pressure.

Circular dichroism (CD) measurements were performed with a MOS-450 biological spectrophotometer (Bio-Logic SAS, Claix, France) fitted out with a 1.0 cm path length cell. Titrations were carried out at 25 °C by adding increasing amounts of the dye to the polynucleotide solution. Spectrograms were obtained in the 200−800 nm range at 2 nm/s speed. CD thermal stability measurements were carried out in the 30−80 °C range; the system was allowed to stabilize for 5 min at the working temperature. Molar ellipticity (deg M_{BP}^{-1} cm^{-1}) was calculated using $[\theta] = 100\theta/C_P l$, where C_P is the polynucleotide concentration (M_{BP}) and l is the cell light path (cm).

Viscosity measurements were performed using a Micro-Ubbelohde viscometer whose temperature was controlled by an external thermostat (25 ± 0.1 °C). The viscosity data were analyzed using $\eta/\eta_0 = (t - t_0)/(t_{DNA} - t_0)$, where t_0 and t_{DNA} are the solvent and polynucleotide solution flow times, respectively, whereas t is the flow time of the thionine and DNA mixture. Mean values of replicated measurements were used to evaluate the sample viscosity, η, and that of DNA alone, η_0.[32]

Kinetics experiments were carried out using a Dialog T-jump instrument in the fluorescence mode (λ_{exc} = 565 nm and λ_{emi} = 620 nm). To minimize thionine photobleaching, the sample was illuminated only during the short time period needed for measurements. The dependence rate on the reactants concentration has been investigated by varying both thionine and polynucleotide concentrations. The kinetic curves were collected by an Agilent DSO6032A (Palo Alto, CA) storage oscilloscope, transferred to a computer, and analyzed with the fitting package by Jandel (AISN software, Mapleton, OR). Each shot was repeated at least eight times, and the resulting relaxation curves were achieved by accumulation.

3. RESULTS

3.1. Equilibria. The binding of thionine to the three RNA structures used can be represented by the apparent reaction 1:

$$P + D \overset{K_{app}}{\rightleftharpoons} PD \qquad (1)$$

dx.doi.org/10.1021/jp307840c | J. Phys. Chem. B 2013, 117, 38−48

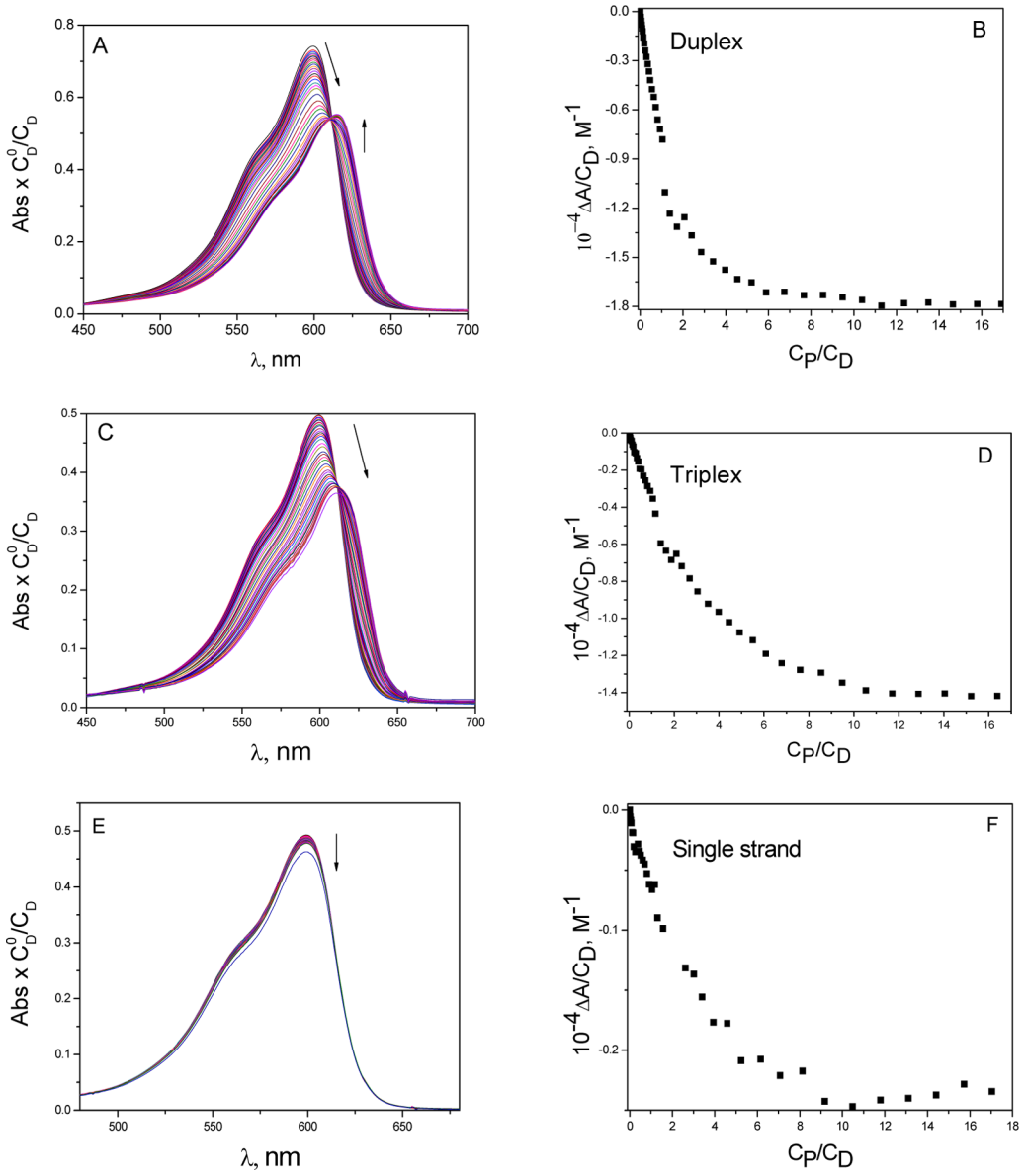

Figure 2. Absorbance spectra corrected by dilution ($C_D°/C_D$) and binding isotherms for the titration of thionine with duplex (A and B), $C_D°$ = 1.37 × 10^{-5} M, triplex (C and D), $C_D°$ = 1.22 × 10^{-5} M, and single strand (E and F), $C_D°$ = 1.22 × 10^{-5} M. λ_{max} = 600 nm, I = 0.1 M (NaCl), pH = 7.0, and T = 25 °C.

where P denotes the poly(rU) (single strand, ss), poly(rA)·poly(rU) (duplex), and poly(rA)·2poly(rU) (triplex) polynucleotide free sites, D stands for free thionine, and PD is the complex formed. The equilibrium concentrations will be denoted as [P], [D], and [PD], respectively.

The spectra and binding isotherms for thionine−duplex, thionine−triplex, and thionine−ss are shown in Figure 2A−F. The curves are monophasic at I = 0.1 M. The spectra recorded during the titration of thionine by triplex (Figure 2C) was similar to that described for the titration of thionine by duplex (Figure 2A); a decrease in absorbance intensity at 600 nm, an isosbestic point at 610 nm, and a 12 nm bathochromic shift are observed. Even fewer spectral changes were observed for thionine−ss, with only a hypochromic effect at 600 nm devoid of isosbestic point (Figure 2E).

At the lowest ionic strength used, I = 0.01 M, two different processes were observed as the C_P/C_D ratio was raised (Supporting Information Figure 1SI). When the ionic strength was increased up to 1 M (data not shown), the salt effect makes the data analysis difficult, as long as ionic strength clearly affects the interaction of thionine with double-stranded RNA, indicating the significance of electrostatic interactions; electrostatics plays a key role in the intercalation of cationic ligands.[33,34]

For all the systems studied, the interaction could be represented by reaction 1, except for thionine−duplex at I = 0.01 M (Supporting Information Figure 1SI). In this case, a more precise analysis of the biphasic isotherm was unfeasible, even after splitting the isotherm into two realms: a first from C_P/C_D = 0−1.0, showing a decrease in absorbance intensity at λ = 600 nm, and a second from C_P/C_D = 1.0−11, in which a hyperchromic effect is observed. The CD spectral curves displayed two types of complex species (see below), intercalated and external, corresponding to each realm.

The fluorescence spectra for thionine−duplex and thionine−triplex are collected in Supporting Information Figure 2SI along

dx.doi.org/10.1021/jp307840c | J. Phys. Chem. B 2013, 117, 38−48

Table 1. Binding Constants and Site-Size Parameter, *n*, Obtained for Thionine−Duplex, Thionine−Triplex, and Thionine−ss with Eq 2[a]

thionine−duplex			thionine−triplex			thionine−ss	
n	$10^{-5} \times K_{app}$, M^{-1}[b]	$10^{-5} \times K_{app}$, M^{-1}[c]	n	$10^{-4} \times K_{app}$, M^{-1}[b]	$10^{-3} \times K_{app}$, M^{-1}[c]	n	$10^{-5} \times K_{app}$, M^{-1}[b]
1	1.2 ± 0.15	1.1 ± 0.02	2	3.7 ± 0.23	6.0 ± 0.33	2	3.7 ± 0.57

[a] I = 0.1 M (NaCl), pH = 7.0, and T = 25.0 °C. [b] Absorbance titration. [c] Fluorescence titration.

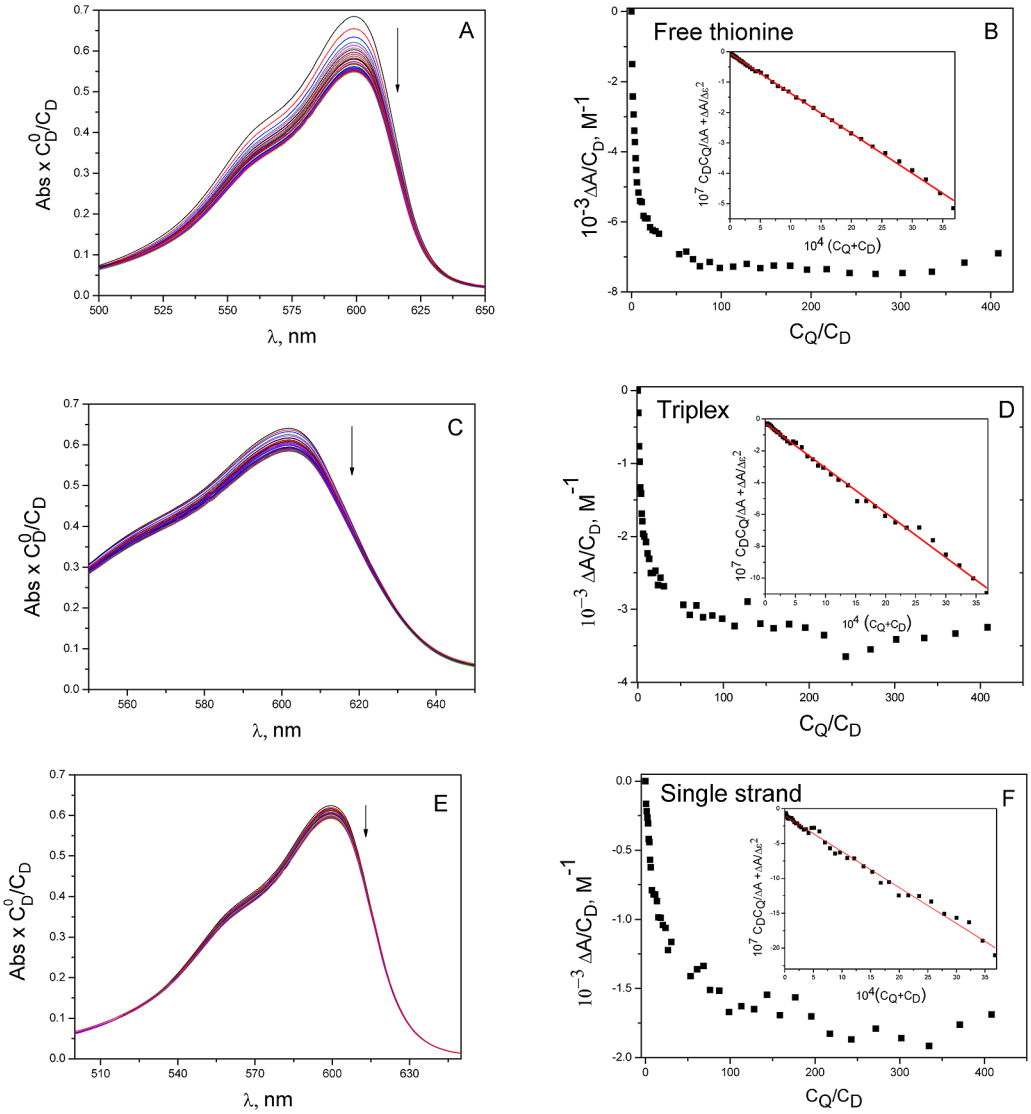

Figure 3. Absorption spectra (A, C, and E), binding isotherms (B, D, and F), and inset eq 4 plot obtained for (A and B) thionine/$Fe(CN)_6]^{4-}$, (C and D) thionine−triplex/$Fe(CN)_6]^{4-}$, and (E and F) thionine−ss/$Fe(CN)_6]^{4-}$. C_D/C_P = 0.1. C_Q = 1.00 × 10^{-2} M, C_D = 1.37 × 10^{-5} M. λ = 600 nm, I = 0.1 M (NaCl), pH = 7.0, and T = 25 °C.

with the corresponding binding isotherms, which were monophasic. The fluorescence of thionine upon interaction with the duplex is quenched compared to triplex. For thionine−duplex, only a decrease in the fluorescence intensity was observed, whereas for the triple helix the decrease is accompanied by a 10 nm red shift. This behavior differs from that observed with other aminoacridines like proflavine,[28] in which a fluorescence increase is observed upon addition of duplex and triplex.

Except for thionine−ss (whose fluorescence isotherm could not be analyzed), the binding constants were evaluated from the absorbance and fluorescence experiments at I = 0.1 M using the McGhee and von Hippel equation:[35]

$$\frac{C_D}{\Delta A} = \frac{1}{\Delta \varepsilon^2} + \frac{1}{K_{app}\Delta \varepsilon}\frac{1}{[P]} \quad (2)$$

where [P] stands for the equilibrium polynucleotide concentration calculated from the expression $[P] = C_P f(r)$, where $f(r) = (1 - nr)^n/[1 - (n - 1) - r]^{(1-n)}$, r being the ratio of the bound to free polynucleotide. The site size (n), the number of base pairs occupied by a single dye molecule upon binding, was calculated at low ionic strength, in which the complex is quantitatively formed. The intersection of the first realm of the

dx.doi.org/10.1021/jp307840c | J. Phys. Chem. B 2013, 117, 38−48

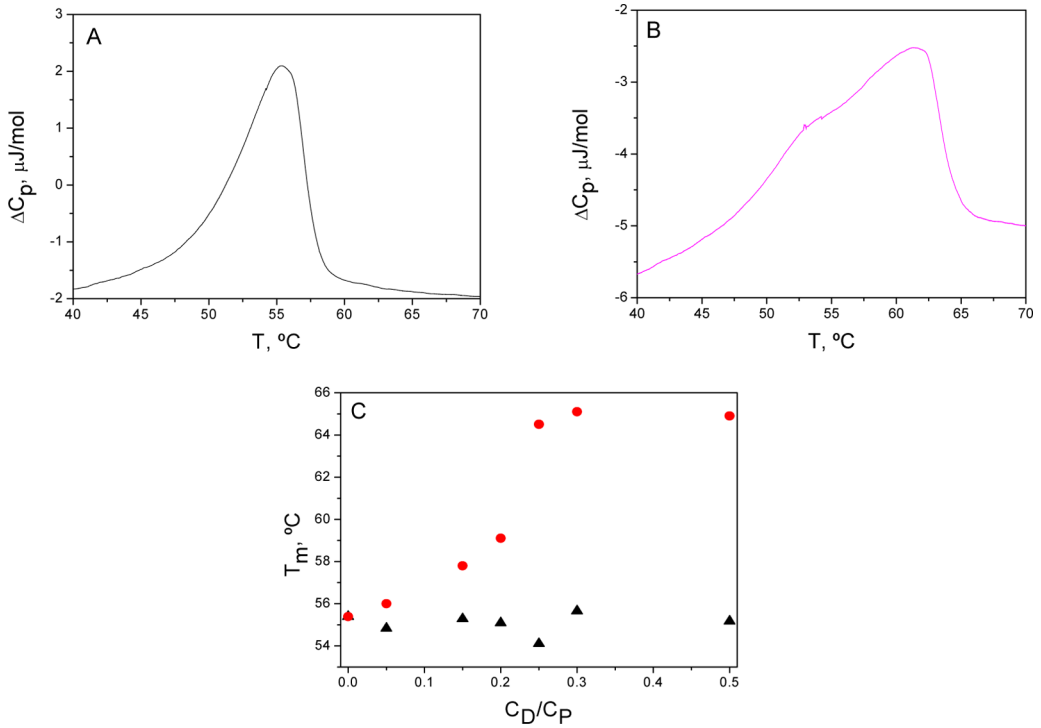

Figure 4. DSC melting plots for thionine–duplex: (A) $C_D/C_P = 0$; (B) $C_D/C_P = 0.25$. $C_P = 4.00 \times 10^{-4}$ M; scan rate, 1 °C/min; $P = 3$ atm; pH = 7.0; $I = 0.1$ M (NaCl). (C) T_m vs C_D/C_P: (▲) T_{mF}, (●) T_{mD}.

two branches of the titration curve yields the value of n on the X axis. The $C_D/\Delta A$ versus $1/[P]$ plot yields the K_{app} value by an iteration procedure. ΔA is calculated as $A - A_0$, A and A_0 being the absorbance of the dye in the presence of polynucleotide and the absorbance of the dye alone, and $\Delta\varepsilon = \varepsilon_{PD} - \varepsilon_D$; note that in fluorescence experiments ΔA and $\Delta\varepsilon$ are replaced by ΔF and $\Delta\varphi$, respectively. Supporting Information Figure 3SI shows the McGhee and von Hippel fitting, and Table 1 collects the binding constants obtained.

3.2. Quenching. Quenching experiments constitute a reliable method to investigate the binding of nucleic acids and proteins. Quenching measurements were performed by adding increasing amounts of $K_4[Fe(CN)]_6$ to a constant free dye content in solution or bound to RNA in single strand, or double or triple helices. Thus, four sets of experiments were performed: thionine–ss, thionine–duplex, and thionine–triplex, all of them at $C_D/C_P = 0.1$, and free thionine as well. The F_0/F versus $K_4[Fe(CN)]_6$ data pairs were plotted (Supporting Information Figure 4SI) according to the Stern–Volmer equation $F_0/F = 1 + K_{SV}[Q]$ being the quencher concentration and F_0 and F the fluorescence emission intensity in the absence and in the presence of quencher, respectively. The nonlinear behavior observed even at the lowest quencher content reveals a complex behavior that entails different processes.

To gain a deeper insight onto possible quenching processes, the absorption spectra were recorded during the titration with $K_4[Fe(CN)]_6$ under the same conditions of the quenching experiments. The results corresponding to the interaction of the quencher with free thionine, thionine–triplex, and thionine–ss at $C_D/C_P = 0.1$ are shown in Figure 3, parts A, C, and E. No spectral changes were observed on addition of $K_4[Fe(CN)]_6$ to thionine–duplex at $C_D/C_P = 0.1$. This behavior reveals that ferrocyanide reacts with all three free thionine, thionine–ss, and thionine–triplex, whereas it does not react with thionine–duplex. Parts B, D, and F of Figure 3 plot the binding isotherms, and the inset shows the graphical fittings to eq 3:

$$\frac{C_D C_Q}{\Delta A} + \frac{\Delta A}{\Delta\varepsilon^2} = \frac{1}{K_Q \Delta\varepsilon} + \frac{C_D + C_Q}{\Delta\varepsilon} \quad (3)$$

The fluorophore–quencher formation constant, K_Q, was evaluated from the intercept. The values obtained at pH = 7.0, $I = 0.1$ M were $K_Q = (2.2 \pm 0.4) \times 10^4$ M^{-1} for the thionine/$K_4[Fe(CN)]_6$ binary system and for the ternary systems $K_Q = (1.1 \pm 0.2) \times 10^4$ M^{-1} for thionine–triplex/$K_4[Fe(CN)]_6$ and $K_Q = (5.1 \pm 0.7) \times 10^3$ M^{-1} for thionine–ss/$K_4[Fe(CN)]_6$.

The similar values obtained for the K_Q constants of ferrocyanide/free thionine system and ferrocyanide/thionine–triplex complex suggest that an external thionine–triplex complex is formed. Absence of the ferrocyanide/thionine–duplex ternary complex is explained by the greater thionine affinity with the duplex compared to ferrocyanide (Table 1), and because the intercalated site does not favor the formation of the ternary complex. Summarizing, under the $C_D/C_P = 0.1$ conditions, only the free and external bound thionine in thionine–triplex and, to less extent, in thionine–ss are able to form complexes with ferrocyanide. A dynamic quenching effect must characterize the ferrocyanide complex, because the fluorescence diminishes in the presence of the polynucleotide (either duplex or triplex) with respect to free thionine (Supporting Information Figure 2SI).

3.3. Thermal Stability. The thionine effect on the thermal stability of the double and triple helices was evaluated by DSC. When thionine was added to duplex and the C_D/C_P ratio was raised, the denaturation process yielded two peaks. Parts A and B of Figure 4 show the evolution of the calorimetric curves for thionine–duplex at 0 and 0.25 C_D/C_P ratio. Two peaks appeared as the C_D/C_P ratio was raised from 0.15 to 0.50,

dx.doi.org/10.1021/jp307840c | J. Phys. Chem. B 2013, 117, 38–48

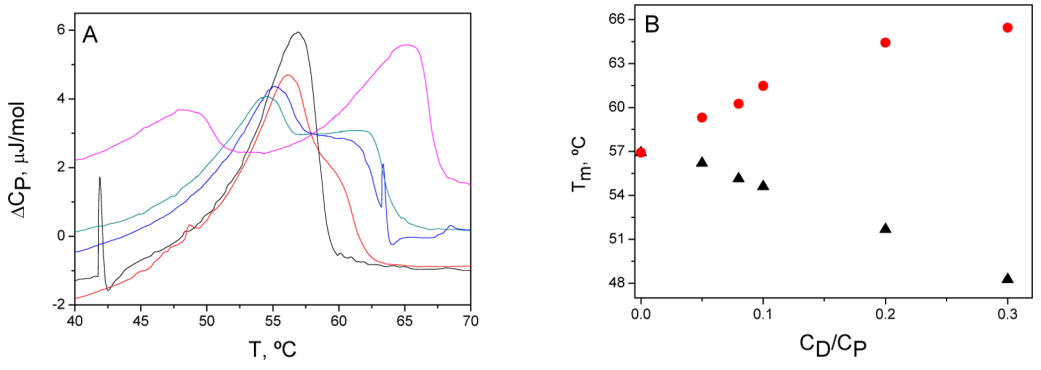

Figure 5. DSC Melting plots for thionine–triplex: C_D/C_P = 0, 0.05, 0.08, 0.1, 0.2, and 0.3. $C_P = 4.00 \times 10^{-4}$ M; scan rate, 1 °C/min; P = 3 atm; pH = 7.0; I = 0.1 M (NaCl); T = 20–90 °C. (B) T_{mD} vs C_D/C_P: (▲) T_{mT}, (●) T_{mD}; I = 0.1 M (NaCl) and pH = 7.0.

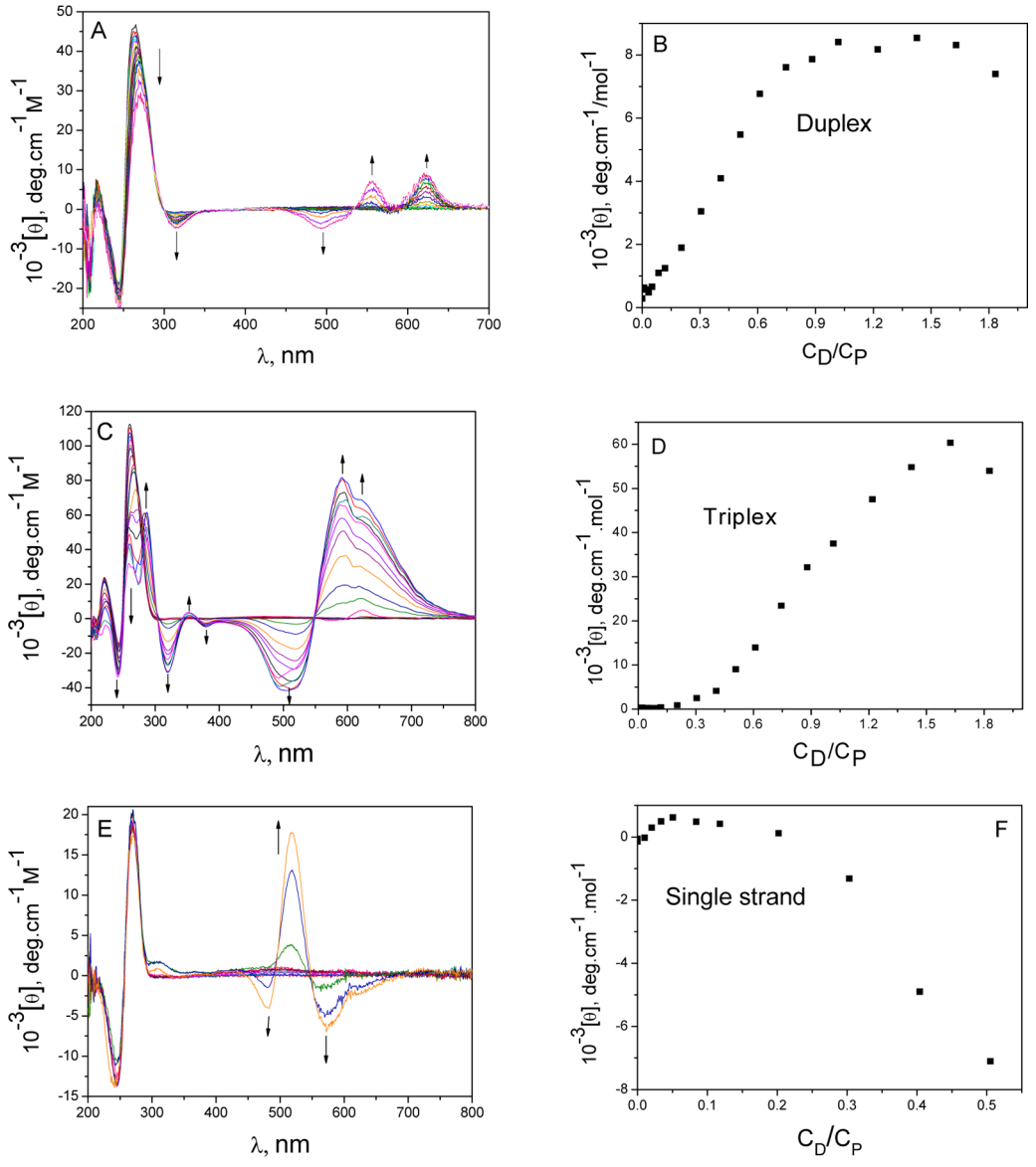

Figure 6. CD spectrograms (A, C, and E) and [θ] vs C_D/C_P plots (B, D, and F) for thionine–duplex (A and B), $C_D = 9.20 \times 10^{-4}$ M, λ = 625 nm; thionine–triplex system (C and D), $C_D = 9.00 \times 10^{-4}$ M, λ = 625 nm; thionine–ss (E and F), $C_D = 9.00 \times 10^{-4}$ M, λ = 572 nm. I = 0.1 M (NaCl), pH = 7.0, and T = 25 °C.

revealing two melting processes. The left peak is assigned to melting of free duplex because the melting temperature (T_{mF}) was independent of the C_D/C_P ratio; the right peak corresponds to denaturation of the duplex thionine–duplex to yield thionine–poly(rU) + thionine–poly(rA), T_{mD} being melting temperature. The T_{mD} value rose in 10 °C steps up to C_D/C_P =

dx.doi.org/10.1021/jp307840c | J. Phys. Chem. B 2013, 117, 38–48

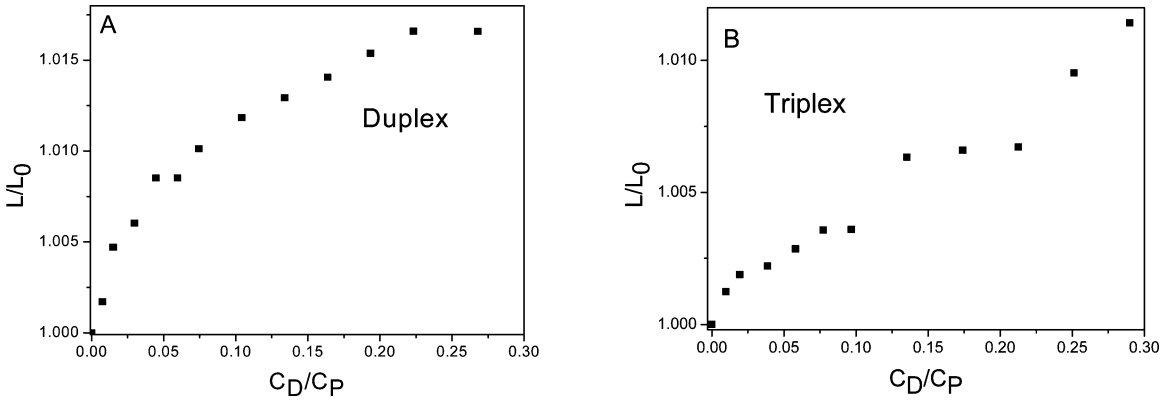

Figure 7. Relative contour length obtained for (A) thionine–duplex, $C_D = 1.00 \times 10^{-3}$ M, $I = 0.1$ M, and (B) thionine–triplex, $C_D = 1.16 \times 10^{-3}$ M, $I = 0.1$ M (NaCl), pH = 7.0, and $T = 25$ °C.

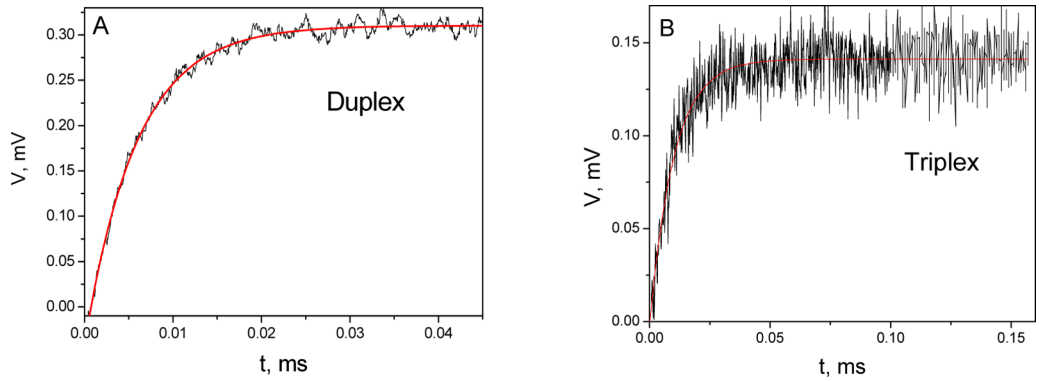

Figure 8. T-jump curve for thionine–duplex (A) $C_D^0 = 5.50 \times 10^{-4}$ M, $C_P^0 = 1.40 \times 10^{-3}$ M, and for thionine–triplex (B) $C_D^0 = 5.50 \times 10^{-4}$ M, $C_P^0 = 2.52 \times 10^{-3}$ M. $I = 0.1$ M (NaCl), pH = 7.0, and $T = 25$ °C.

0.25 (Figure 4C); such a T_{mD} increase is typical of intercalation reactions displaying thermal stabilization of the system.[27]

The melting temperature (T_{mT}) of the triple stranded RNA was 57 °C in the absence of thionine. When the thionine content was raised, two bands appeared that stepwise moved apart. The intensity of the right-hand band rose, while dropping that of the left-hand band; the set of DSC melting plots yielded an "isocaloric point" with constant heat capacity, denoting that a reaction at equilibrium governed by the thionine content is at work (Figure 5A). The maximum of the right-hand band adopts the same increase profile as that for T_{mD} of the thionine–duplex intercalated complex, outlined by the stretch of rising temperature (Figure 4C), that is, thionine causes the formation of the thionine–duplex complex from thionine–triplex. Likewise, the drop in the melting temperature, T_{mT}, for thionine–triplex (Figure 5B) reveals the formation of an external complex, most likely linked to the groove.[36]

3.4. CD Measurements. The data gathered point to dye/polynucleotide interactions that alter the achiral environment of thionine, giving rise to induced circular dichroism (ICD) in agreement with the conformational change of the polynucleotide structure. The spectrograms recorded are strongly dependent on the ionic strength, consistent with observations by Kamiya.[37] Supporting Information Figure 5SI shows the spectrogram and titration isotherm of thionine–duplex at $I = 0.01$ M. Five different bands are observed in the ICD, three negative at $\lambda = 313$, 495. and 580 nm, and two positive at $\lambda = 551$ and 620 nm, as well as two isodichroic points at 511 and 565 nm. At $I = 0.1$ M (Figure 6A), two isodichroic points appeared at $\lambda = 534$ and 594 nm. The plot of the molar ellipticity at 625 nm versus C_D/C_P (Supporting Information Figure 5SIB and Figure 6B) shows an inflection point at $C_D/C_P = 0.75$ and $I = 0.01$ M that correlates fairly well with the saturation of the single complex observed at $I = 0.1$ M. The increase of $[\theta]$ with C_D/C_P corresponds to an intercalation process, and the decrease corresponds to groove binding,[38] revealing that two distinct complexes are formed at $I = 0.01$ M, whereas only a single intercalated complex is formed at $I = 0.1$ M, in good agreement with previous results.

Parts C and D of Figure 6 show the spectrogram and isotherm ($[\theta]$ vs C_D/C_P) for thionine–triplex at $I = 0.1$ M. A complicated pattern is observed that consists of maxima in the ICD region at 352, 595, and 620 nm, minima at 319, 380, and 520, and an isodichroic point at 594 nm. The band at 260 nm vanishes when C_D/C_P is raised, emerging as a new band at 288 nm. The molar ellipticity at 625 nm versus C_D/C_P gives rise to a sigmoid curve that resembles a titration curve.

No bathochromic effect was observed for thionine–ss (Figure 6E) at $\lambda = 260$ nm. Two positive bands appeared in the ICD region at 312 and 520 nm and two negative at 482 and 572 nm, giving rise to two isodichroic points at $\lambda = 495$ and 595 nm. The spectrogram probes interaction of thionine with single-stranded RNA, as observed in the absorbance titrations. The $[\theta]$ versus C_D/C_P plot obtained (Figure 6F) differs from that of the double and triple stranded. For the RNA single strand, the inflection point is observed at $C_D/C_P = 0.2$.

3.5. Viscosity Measurements. The viscosity ratio η/η_0, where η_0 is the viscosity of the polymer alone and η is the

dx.doi.org/10.1021/jp307840c | J. Phys. Chem. B 2013, 117, 38–48

viscosity of the dye/polynucleotide system, is related to the elongation of the polynucleotide[39,40] by eq 4:[32]

$$\frac{L}{L_0} = \sqrt[3]{\frac{\eta}{\eta_0}} = 1 + \beta\frac{C_D}{C_P} \quad (4)$$

where L is the contour length of the dye/polynucleotide system, L_0 is that of the free polynucleotide, and β is the slope. L/L_0 was plotted as a function of the C_D/C_P ratio; Figure 7 shows the plot of eq 4 at I = 0.1 M. Precipitation of thionine has prevented us from arriving only up to C_D/C_P = 0.28; the plot describes a downward curve, probably due to saturation of the polynucleotide free sites at high C_D/C_P ratio. These results concur with the intercalative binding of thionine into the double helix.[32] For triplex, the L/L_0 versus C_D/C_P plot is similar to that of the duplex, even though the initial slope of the isotherm is clearly different and no saturation of polynucleotide is observed up to C_D/C_P = 0.3.

3.6. Kinetic Study. The binding of thionine with the double and triple RNA helices was studied by the T-jump technique in the fluorescence mode. The resulting curves were all single exponential (Figure 8, parts A and B). The reciprocal of the relaxation time as a function of the concentration term ([P] + [D]) gives rise to a single straight line (Figure 9),

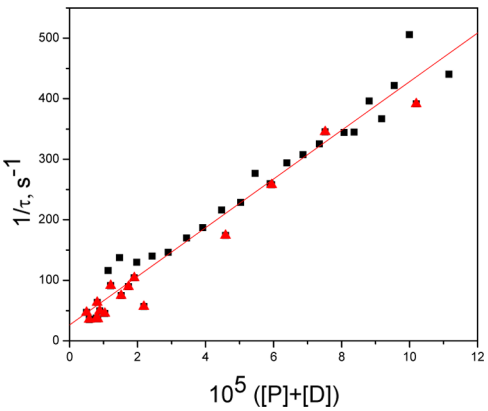

Figure 9. $1/\tau$ vs ([P] + [D]) plot for thionine−duplex (■) $C_D^0 = 5.50 \times 10^{-4}$ M, $C_P^0 = 1.40 \times 10^{-3}$ M, and for thionine−triplex, (▲) $C_D^0 = 5.50 \times 10^{-4}$ M, $C_P^0 = 2.52 \times 10^{-3}$ M. I = 0.1 M (NaCl), pH = 7.0, and T = 25 °C.

suggesting that the reaction mechanism corresponding to thionine interaction with duplex and triplex RNA occurs in a single step, consistent with eq 5. The equilibrium concentration values for the triplex were determined from the highest K_{app} value (Table 1) because, as seen above, the triplex partially converts into the duplex under the experimental conditions and therefore the constant embraces both processes.

$$1/\tau = k_1([P] + [D]) + k_{-1} \quad (5)$$

The apparent equilibrium constant, K_{app}, can be calculated as the ratio between the formation constant (k_f) and the dissociation constant (k_d). The K_{app} (Table 2) coincides with the binding constant for thionine−duplex deduced statically (Table 1), which supports preceding results, bearing out the isothermal denaturation reaction. It should be recalled that the formation and dissociation rates of the complexes formed by groove binding are too fast to be observed by T-jump. Therefore, the kinetic results unambiguously show that, starting from either duplex or triplex, an intercalation reaction is observed, and this corresponds to binding to the duplex.

Table 2. Formation Constants, k_f, Dissociation Constants, k_d, and Equilibrium Constant, K_{app}, Obtained for Thionine−Duplex and Thionine−Triplex[a]

	thionine−duplex and thionine−triplex
k_f	$(4.02 \pm 0.13) \times 10^6$, M^{-1} s^{-1}
k_d	26.27 ± 7.40, s^{-1}
$K_{app} = k_f/k_d$	$(1.53 \pm 0.18) \times 10^5$, M^{-1}

[a] I = 0.1 M (NaCl), pH = 7.0, and T = 25 °C.

4. DISCUSSION

Thionine intercalates into duplex RNA. For thionine−duplex, the absorbance and fluorescence experiments led to same K_{app} value, very close to that reported for the formation of the intercalated thionine−dsCT−DNA complex[1] and similar to that for intercalation of ethidium bromide into duplex.[41] The affinity constant for the formation of thionine−ssCT−DNA[1] is an order of magnitude lower than that for thionine−ss. The values deduced for n were much higher for thionine−CT−DNA (n = 5.6 for dsCT−DNA and n = 7.4 for ssCT−DNA)[1] and with synthetic DNA[9] compared to thionine−duplex (Table 1). This means that the thionine−DNA complex reached saturation at a lower concentration ratio than thionine−duplex RNA and thionine−ss. For thionine−triplex, the K_{app} value deduced from absorbance measurements was higher relative to fluorescence measurements (Table 1), a feature to be justified below. In both cases, the binding constant for thionine−triplex was lower relative to the intercalated ethidium−triplex complex.[27] The lowest K_{app} value was closer to that for external binding. The isotherm plotted in Figure 2E and the variation of CD (Figure 6E) demonstrate the interaction of thionine with RNA single strand. The value of the constant 3.7×10^5 M^{-1} is similar to that of the coralyne−poly(rU) system $K = (4.6 \pm 0.5) \times 10^5$ M^{-1} (measured in our laboratory).

The experiments using $K_4[Fe(CN)]_6$ as a quencher are informative. The isotherms shown in Figure 3, parts B, D, and F, disclose the formation of the thionine/$K_4[Fe(CN)]_6$ binary complex and the thionine−triplex/$K_4[Fe(CN)]_6$ and thionine−ss/$K_4[Fe(CN)]_6$ ternary complexes. Formation of the thionine−duplex/$K_4[Fe(CN)]_6$ ternary complex was not observed because the thionine intercalated into duplex is inaccessible to the quencher. These findings reinforce earlier results, that is, the intercalative binding of thionine into duplex RNA and external (most likely groove binding) into triplex RNA. The amplitude of the isotherm recorded for thionine−ss drops to one-fourth relative to free thionine and to one-half relative to thionine−triplex. This result reveals that, at 25 °C and pH = 7.0, poly(rU) is able to generate double helices that intercalate into thionine in a similar way as poly(rA) at 25 °C and pH = 5.2 in the presence of proflavine[42] and as poly(rU) in the presence of coralyne at 25 °C and pH = 7.0 (data not published). The smaller amplitude of the triplex curve with respect to free thionine can be interpreted on the basis of reaction 6 (see below), in which a certain portion of thionine remains as intercalated thionine−duplex under the experimental conditions used.

In good agreement with the results discussed above, the DSC experiments clearly show two types of binding of thionine to the duplex and triplex. In the case of thionine−duplex, Figure 4C shows that the melting temperature (T_{mD}) increases when

dx.doi.org/10.1021/jp307840c | J. Phys. Chem. B 2013, 117, 38−48

the C_D/C_P ratio is raised, revealing that thionine stabilizes the double helix, this behavior being characteristic of the intercalative binding;[38] also is shown a melting temperature (T_{mF}) independent of the thionine concentration, which corresponds to the melting of the free duplex present in solution.

A different behavior is observed for thionine−triplex. When increasing amounts of thionine were added to triplex, two bands related to the denaturation according to a two-step process appeared (Figure 5A) whose maxima progressively moved apart.

Figure 5B shows the evolution of the T_{mT} and T_{mD} values for the two bands which correspond to the denaturation temperature for thionine−triplex → thionine−duplex + thionine−poly(rU) and for thionine−duplex → thionine−poly(rA) + thionine−poly(rU), respectively.

Formation of thionine−poly(rA) is a reasonable assumption as long as at pH = 7.0 poly(rA) displays great affinity with intercalants, as occurs with coralyne.[29] Figure 5B shows that the trend of the increase in T_{mD} is similar to that observed for thionine−duplex (Figure 4C), that is, thionine intercalates into the duplex emerging from the triplex thermal denaturation. On the contrary, T_{mT} diminishes when the thionine content is raised; in other words, thionine destabilizes the triple helix as a consequence of the groove binding.[36] This behavior has been observed also with ethidium bromide.[27] However, the thionine−triplex system displays a singular behavior (the presence of an isocaloric point) which, to the best of our knowledge, has not been reported hitherto for other systems. Figure 5A shows that the area of the right-hand band increases while that of the left-hand band diminishes. The former is related to the amount of thionine−triplex and the latter with thionine−duplex initially present in solution. In other words, when the thionine content is raised, the percentage of the thionine−triplex complex present in solution at 25 °C diminishes and that of the thionine−duplex increases, the observed isocaloric point denoting that both species are in equilibrium.

These findings, reinforced below by other techniques, reveal that the thionine bound to triplex brings about the isothermal denaturation of the triplex (T = 25 °C), according to the reaction scheme:

$$\text{thionine−triplex} + \text{thionine} \overset{K_D}{\rightleftharpoons} \text{thionine−duplex} + \text{thionine−ss} \quad (6)$$

K_D being the isothermal denaturation constant for equilibrium 6, which shifts to right upon increasing the thionine content, as inferred also from the evolution of the surface of the band areas of Figure 5. Such a behavior is justified by the rather high formation constants for thionine−duplex and thionine−ss relative to thionine−triplex. From the formation constants of the different complexes (Table 1), $K_1 = 6.0 \times 10^3$ M^{-1} for thionine−triplex, $K_2 = 1.1 \times 10^5$ M^{-1} for thionine−duplex, and $K_3 = 3.7 \times 10^5$ M^{-1} for thionine−ss, it follows $K_D = 522$ calculated as $(K_2)(K_3/K_1)(K_{f,T})$, the formation constant of triplex from duplex and ss being $K_{f,T} = 1.3 \times 10^4$ M^{-1}. The $K_{f,T}$ value deduced from kinetic measurements[43] at 0.011 M (NaCl) ionic strength was corrected for 0.1 M (NaCl).[44] This value was (roughly) an order of magnitude lower than that reported for the formation constant of oligonucleotides DNA triplex[45] quencher.

The difference in the K_{app} values deduced from absorbance and fluorescence measurements for the formation constant of the thionine−triplex complex can now be explained by the larger thionine content in the former case and hence by the greater conversion to duplex, reflected in a higher equilibrium constant. Typically, the interaction of an intercalating reagent with DNA is characterized by following the hypochromism and bathochromic shift associated with the binding of the ligand to the duplex.[46] These effects, observed in Figure 2, parts A and C, demonstrate the presence of intercalated complexes in the two absorbance experiments, thionine−duplex and thionine−triplex. For this reason, we chose the lower constant value obtained from fluorescence measurements as the representative value of the formation constant for the thionine−triplex external complex.[36]

The isothermal denaturation also justifies the CD, viscometric, and kinetic results obtained at T = 25 °C. Formation of the intercalated thionine−duplex complex from the groove thionine−triplex complex according to eq 6 is also reflected in Figure 6D by the initial induction period and further rise of $[\theta]$ according to the same pattern as that of thionine−duplex (Figure 6B). The observed increase in viscosity in Figure 7A is related to the intercalative binding of thionine to the duplex, because the increase in viscosity bears relation with the helix lengthening due to intercalation. However, the rise in viscosity (Figure 6B), observable for $C_D/C_P > 0.1$, is not justified by the groove binding in thionine−triplex; rather, this behavior is related to formation of the thionine−duplex intercalated complex consistent with the isothermal denaturation and the experiments discussed above.

Finally, the kinetic experiments are conclusive. Given that thionine−duplex and thionine−triplex systems lead to the same kinetic results and in view that groove binding complexes form too rapidly to be observed by T-jump, we can then conclude that the kinetic experiments of the thionine−triplex system refer to the intercalation reaction of thionine into the duplex present in the system in accordance with the denaturation equilibrium, eq 6.

The final question is, why does reaction 6 occur? Several factors favor this reaction. To a first place, thionine competes with the third strand by destabilizing the triplex. That is particularly true if one considers that the constant for the ss−duplex system ($K_{f,T} = 1.3 \times 10^4$ M^{-1})[37] is less than the intercalated thionine−duplex ($K_{app} = 1.2 \times 10^5$ M^{-1}) (Table 1). Therefore, destabilization of the triplex will occur only with those ligands that, once located in the groove of the triplex, can compete with the poly(rU) single strand for the duplex. At large, this event will occur if the ligand (as it happens with thionine) possesses more affinity with the duplex than with the triplex (Table 1) at the same time it intercalates into the duplex through the major groove. Being the major groove occupied by the third strand, it impedes intercalation, favoring the denaturation. If the ligand were able to intercalate through the minor groove, then it could yield a stable intercalated with the triplex. It can then be surmised that the thionine−duplex complex is formed by intercalation of thionine through the major groove. We have reported earlier that intercalants as representative as proflavine[28] or ethidium bromide[27] tend to destabilize the triplex helix at T > 37 °C; in both systems denaturation was not observed at low temperature. In the case of thionine, the isocaloric point of Figure 5A is indicative of the equilibrium reaction 6, which will only be feasible due to the relative stabilities of the different thionine−RNA complexes at

dx.doi.org/10.1021/jp307840c | J. Phys. Chem. B 2013, 117, 38−48

T = 25 °C. The interpretation described above is consistent with the sets of experimental results collected.

It must be underscored that the process represented by eq 6 differs from the disproportionation of the duplex into triplex and a single strand brought about by coralyne, according to the reaction 2(coralyne−duplex) → coralyne−triplex + coralyne−poly(A); this small crescent-shaped molecule can cause the irreversible disproportionation both for poly(rA)·poly(rU)[29] and poly(dA)·poly(dT).[47] For coralyne−duplex we put forward earlier,[29] the formation of an intermediate quadruplex by the merger of two partially intercalated coralyne−duplexes. Moreover, we have verified that coralyne intercalates into the triplex with great affinity. Thionine, on the contrary, intercalates only into the duplex and binds the major groove in the triplex. This behavior and the different affinity of the dye with the triplex, duplex, and single strands[29] are the reason for the isothermal denaturation of the triplex with thionine (eq 6) and the disproportionation of the duplex with coralyne.

In summary, despite the wide slate of existing studies underlining the main features that can predict the type of binding of an organic molecule to DNA and/or RNA, the experimental reality is that each dye molecule behaves differently, and a puzzle of data must be rationalized to propose convincingly the reaction mechanism with the duplex or the triplex.

5. CONCLUSIONS

Thionine interacts with duplex RNA in a similar way as it does with DNA, working as an intercalating agent. In the presence of triplex RNA, the thionine units located in the major groove can compete with poly(rU) for the duplex, bringing about thermal denaturation of the thionine−triplex complex. The type of binding and the relative affinity of the thionine−triplex, thionine−duplex, and thionine−ss complexes cause that at 25 °C an equilibrium is reached in which it is the thionine concentration, not the temperature, that governs the triplex helix denaturation. This behavior was not observed with other drugs, not even with acridines of similar structure such as proflavine, endowed with a nitrogen atom instead of sulfur atom; that is, the S atom appears to be responsible for the observed DSC equilibrium, an effect borne out also with the other static and dynamic techniques used in this work.

■ ASSOCIATED CONTENT

Supporting Information

Absorbance spectra and binding isotherm for the thionine titration with duplex at I = 0.01 M (NaCl); fluorescence spectrograms and binding isotherms of the titrations of thionine by duplex and by triplex; absorbance and fluoresce titrations analysis according to eq 2; Stern−Volmer plots of free thionine, thionine single-strand, thionine−duplex, and thionine−triplex; circular dichroism spectra and molar ellipticity at λ = 625 nm vs C_D/C_P of thionine−duplex system. This material is available free of charge via the Internet at http://pubs.acs.org.

■ AUTHOR INFORMATION

Notes

The authors declare no competing financial interest.

■ ACKNOWLEDGMENTS

The financial support by the Ministerio de Educación y Ciencia, project CTQ2009-13051/BQU, supported by FEDER, Junta de Castilla y León, project BU-299A12-1, and Caja de Burgos, Spain, is gratefully acknowledged.

■ REFERENCES

(1) Paul, P.; Kumar, G. S. *J. Fluoresc.* **2012**, *22*, 71−80.
(2) Ferguson, L. R.; Denny, W. A. *Mutat. Res., Fundam. Mol. Mech. Mutagen.* **2007**, *623*, 14−23.
(3) Rabinowitch, E.; Epstein, L. F. *J. Am. Chem. Soc.* **1941**, *63*, 69−78.
(4) Tuite, E. M.; Kelly, J. M. *J. Photochem. Photobiol., B* **1993**, *21*, 103−124.
(5) Brown, J. P.; Brown, R. J. *Mutat. Res., Rev. Genet. Toxicol.* **1976**, *40*, 203−224.
(6) Dohno, C.; Stemp, E. D. A.; Barton, J. K. *J. Am. Chem. Soc.* **2003**, *125*, 9586−9587.
(7) Xie, Y.; Chen, A.; Du, D.; Lin, Y. *Anal. Chim. Acta* **2011**, *699*, 44−48.
(8) Paul, P.; Hossain, M.; Suresh Kumar, G. *J. Chem. Thermodyn.* **2011**, *43*, 1036−1043.
(9) Paul, P.; Kumar, G. S. *J. Hazard. Mater.* **2010**, *184*, 620−626.
(10) Hecht, C.; Friedrich, J.; Chang, T.-C. *J. Phys. Chem. B* **2004**, *108*, 10241−10244.
(11) Tor, Y. *ChemBioChem* **2003**, *4*, 998−1007.
(12) Chow, C. S.; Bogdan, F. M. *Chem. Rev.* **1997**, *97*, 1489−1514.
(13) Wilson, W. D.; Ratmeyer, L.; Zhao, M.; Strekowski, L.; Boykin, D. *Biochemistry* **1993**, *32*, 4098−4104.
(14) Arnott, S.; Bond, P. J. *Nature (London), New Biol.* **1973**, *244*, 99−101.
(15) Palchaudhuri, R.; Hergenrother, P. J. *Curr. Opin. Biotechnol.* **2007**, *18*, 497−503.
(16) Knauert, M. P.; Glazer, P. M. *Hum. Mol. Genet.* **2001**, *10*, 2243−2251.
(17) Uhlmann, E.; Peyman, A. *Chem. Rev.* **1990**, *90*, 543−584.
(18) Thuong, N. T.; Hélène, C. *Angew. Chem., Int. Ed. Engl.* **1993**, *32*, 666−690.
(19) Sun, J.-S.; Hélène, C. *Curr. Opin. Struct. Biol.* **1993**, *3*, 345−356.
(20) Kan, Y.; Armitage, B.; Schuster, G. B. *Biochemistry* **1997**, *36*, 1461−1466.
(21) Lee, J. S.; Latimer, L. J. P.; Hampel, K. J. *Biochemistry* **1993**, *32*, 5591−5597.
(22) Kukreti, S.; Sun, J.-S.; Garestier, T.; Hélène, C. *Nucleic Acids Res.* **1997**, *25*, 4264−4270.
(23) Shchyolkina, A. K.; Timofeev, E. N.; Lysov, Y. P.; Florentiev, V. L.; Jovin, T. M.; Arndt-Jovin, D. J. *Nucleic Acids Res.* **2001**, *29*, 986−995.
(24) Polak, M.; Hud, N. V. *Nucleic Acids Res.* **2002**, *30*, 983−992.
(25) Lehrman, E. A.; Crothers, D. M. *Nucleic Acids Res.* **1977**, *4*, 1381−1392.
(26) Felsenfeld, G.; Davies, D. R.; Rich, A. *J. Am. Chem. Soc.* **1957**, *79*, 2023−2024.
(27) Garcia, B.; Leal, J. M.; Paiotta, V.; Ibeas, S.; Ruiz, R.; Secco, F.; Venturini, M. *J. Phys. Chem. B* **2006**, *110*, 16131−16138.
(28) García, B.; Leal, J. M.; Paiotta, V.; Ruiz, R.; Secco, F.; Venturini, M. *J. Phys. Chem. B* **2008**, *112*, 7132−7139.
(29) Biver, T.; Boggioni, A.; García, B.; Leal, J. M.; Ruiz, R.; Secco, F.; Venturini, M. *Nucleic Acids Res.* **2010**, *38*, 1697−1710.
(30) Wilson, W. D.; Wang, Y. H.; Kusuma, S.; Chandrasekaran, S.; Boykin, D. W. *Biophys. Chem.* **1986**, *24*, 101−109.
(31) Janik, B. *Physicochemical Characteristics of Oligonucleotides and Polynucleotides*; IFI/Plenum: New York, 1971.
(32) Cohen, G.; Eisenberg, H. *Biopolymers* **1969**, *8*, 45−55.
(33) Cusumano, M.; Giannetto, A. *J. Inorg. Biochem.* **1997**, *65*, 137−144.
(34) Blake, A.; Peacocke, A. R. *Biopolymers* **1968**, *6*, 1225−1253.
(35) McGhee, J. D.; von Hippel, P. H. *J. Mol. Biol.* **1974**, *86*, 469−489.
(36) Ruiz, R.; García, B.; Garcia-Tojal, J.; Busto, N.; Ibeas, S.; Leal, J.; Martins, C.; Gaspar, J. F.; Borrás, J.; Gil-García, R.; González-Álvarez, M. *J. Biol. Inorg. Chem.* **2010**, *15*, 515−532.
(37) Kamiya, M. *Biochim. Biophys. Acta* **1979**, *562*, 70−79.

(38) García, B.; Leal, J. M.; Ruiz, R.; Biver, T.; Secco, F.; Venturini, M. *J. Phys. Chem. B* **2010**, *114*, 8555−8564.
(39) Gopal, M.; Veeranna, S. *J. Photochem. Photobiol., B* **2005**, *81*, 181−189.
(40) Pilch, D. S.; Waring, M. J.; Sun, J.-S.; Rougée, M.; Nguyen, C.-H.; Bisagni, E.; Garestier, T.; Hélène, C. *J. Mol. Biol.* **1993**, *232*, 926−946.
(41) D'Amico, M. L.; Paiotta, V.; Secco, F.; Venturini, M. *J. Phys. Chem. B* **2002**, *106*, 12635−12641.
(42) Ciatto, C.; D'Amico, M. L.; Natile, G.; Secco, F.; Venturini, M. *Biophys. J.* **1999**, *77*, 2717−2724.
(43) Blake, R. D.; Fresco, J. R. *J. Mol. Biol.* **1966**, *19*, 145−160.
(44) Record, M. T.; Anderson, C. F.; Lohman, T. M. *Q. Rev. Biophys.* **1978**, *11*, 103−178.
(45) Lin, M.-C.; Macgregor, R. B. *Biopolymers* **1997**, *42*, 129−132.
(46) Bloomfield, V. A.; Crothers, D. M.; Tinoco, I. *Physical Chemistry of Nucleic Acids*; Harper & Row: New York, 1974.
(47) Jain, S. S.; Polak, M.; Hud, N. V. *Nucleic Acids Res.* **2003**, *31*, 4608−4615.